OMTN, Volume *24*

Supplemental information

Hepatocyte-targeting and microenvironmentally responsive glycolipid-like polymer micelles for gene therapy of hepatitis B

Jing Miao, Xiqin Yang, Xuwei Shang, Zhe Gao, Qian Li, Yun Hong, Jiaying Wu, Tingting Meng, Hong Yuan, and Fuqiang Hu

Supplemental Text

Functional mechanism of DrzBC and DrzBS

As shown in **Figure S1**, the 10-23 DNAzymes DrzBC and DrzBS each consist of 15 deoxynucleosides that can form a catalytic domain as well as 9 deoxynucleosides forming a substrate identification domain. The identification sequence on both sides of the substrate is specific to the RNA substrate, suggesting that 10-23 DNAzymes can specifically combine with a target mRNA. Furthermore, the central catalytic domain cleaves mRNA by targeting the purine-pyrimidine junctions (A·U sites), thereby blocking expression of the corresponding mRNA.

Constructing and evaluating hepatitis B virus (HBV)-infected mice

Healthy male BALB/C mice (n = 54) were injected with 200 μL of 1×10^{11} vg rAAV8-1.3HBV based on the hydrodynamic method and according to the manufacturer's instructions for recombinant adeno-associated virus 8-1.3HBV (PackGene Biotech, Guangdong, China). On days 21 and 28, peripheral blood was sampled and the sera were segregated to detect HBeAg and HBsAg titers using an Architect I4000 chemiluminescence immunoassay analyzer (Abbott Laboratories, Abbott Park, IL, USA). On day 21, the levels of HBeAg and HBsAg in all of the mice were approximately 300–350 S/CO and 3–40 IU/mL, respectively. On day 28, the expression levels of both antigens were stable at the same range. According to the chemiluminescence immunoassay manual, HBeAg ≥ 1.00 S/CO and HBsAg ≥ 0.05 IU/mL indicates antigen-positive. Accordingly, it may be concluded that we have successfully constructed rAAV8-1.3HBV-infected mice, which were then randomly

divided into nine groups (six in each group) and administered with the corresponding preparations as shown in **Figure S5.**

Supplemental Table

Table S1. Characterization of Gal-CSSO polymer micelles.

Micelles	Diameter (nm)	PDI	Zeta potential (mV)	CMC ($\mu g\ mL^{-1}$)	SD%
Gal-CSSO	138.33 ± 3.68	0.29 ± 0.03	16.93 ± 0.42	81.06 ± 1.32	11.91 ± 0.21

PDI, CMC, and SD values represent the polydispersity index, critical micelle concentration, and amino substitution degree, respectively. Data represent the mean ± SD (n = 3).

Supplemental Figures

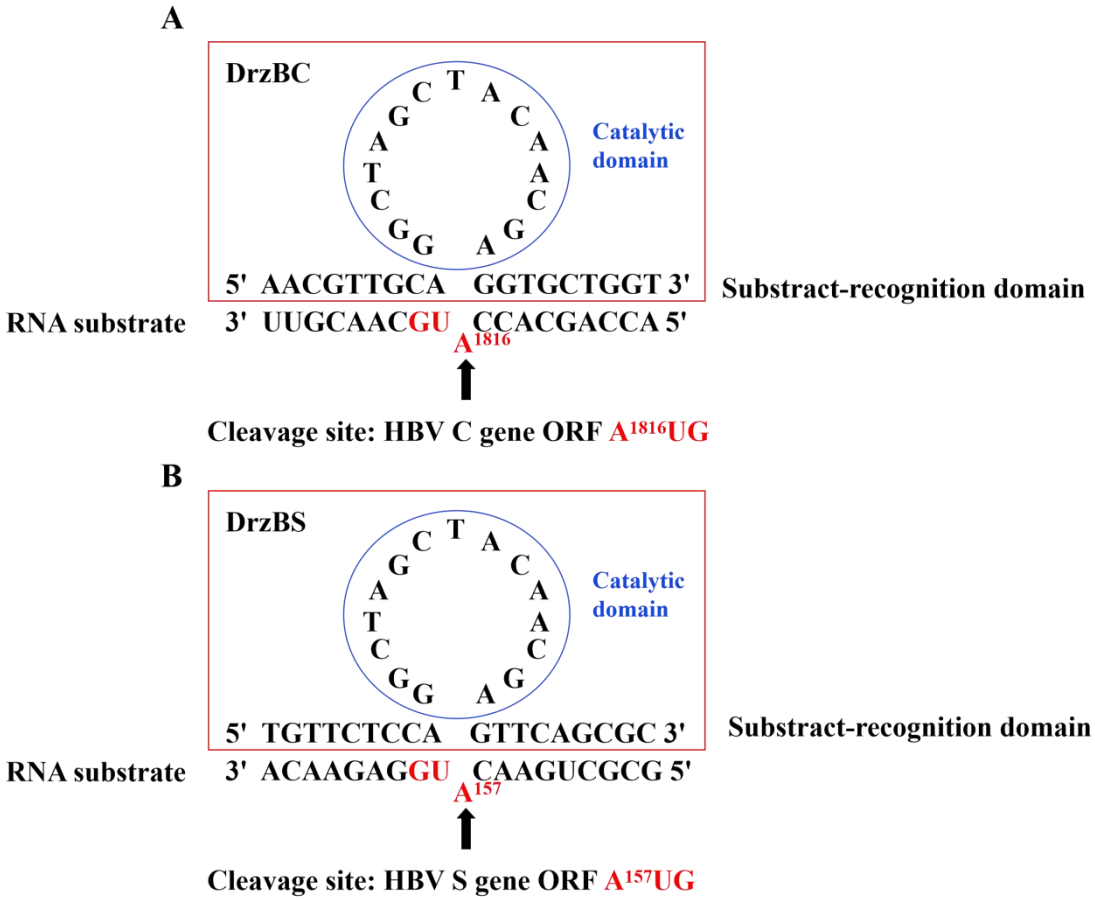

Figure S1. Sequences and molecular structures of DrzBC and DrzBS and their RNA substrates.

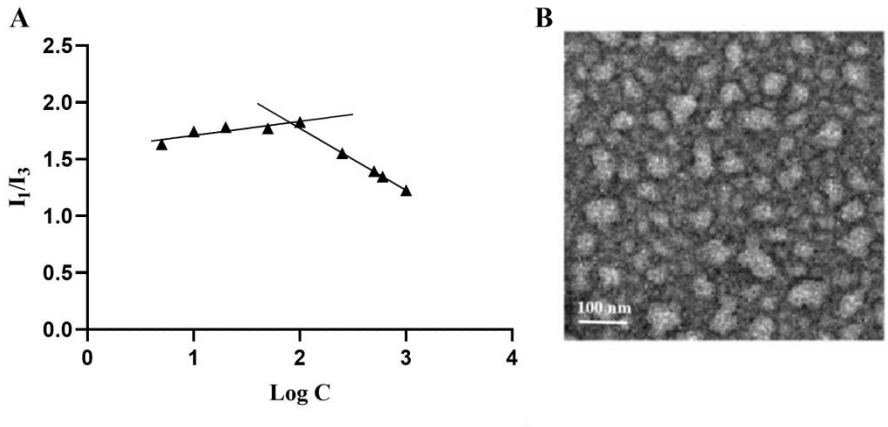

Figure S2. Characterization of Gal-CSSO polymer micelles. (A) Variation of intensity ratio (I_1/I_3) vs. concentration (μg mL^{-1}) of Gal-CSSO (▲). (B) Transmission electron microscopy image of Gal-CSSO. Gal-CSSO, galactosylated chitosan-oligosaccharide-SS-octadecylamine.

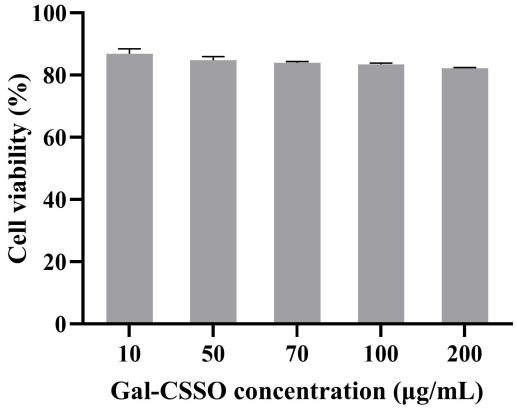

Figure S3. *In vitro* cytotoxicity of Gal-CSSO against HepG2.2.15 cells after treatment for 48 h. Values shown are the mean ± SD (n = 3).

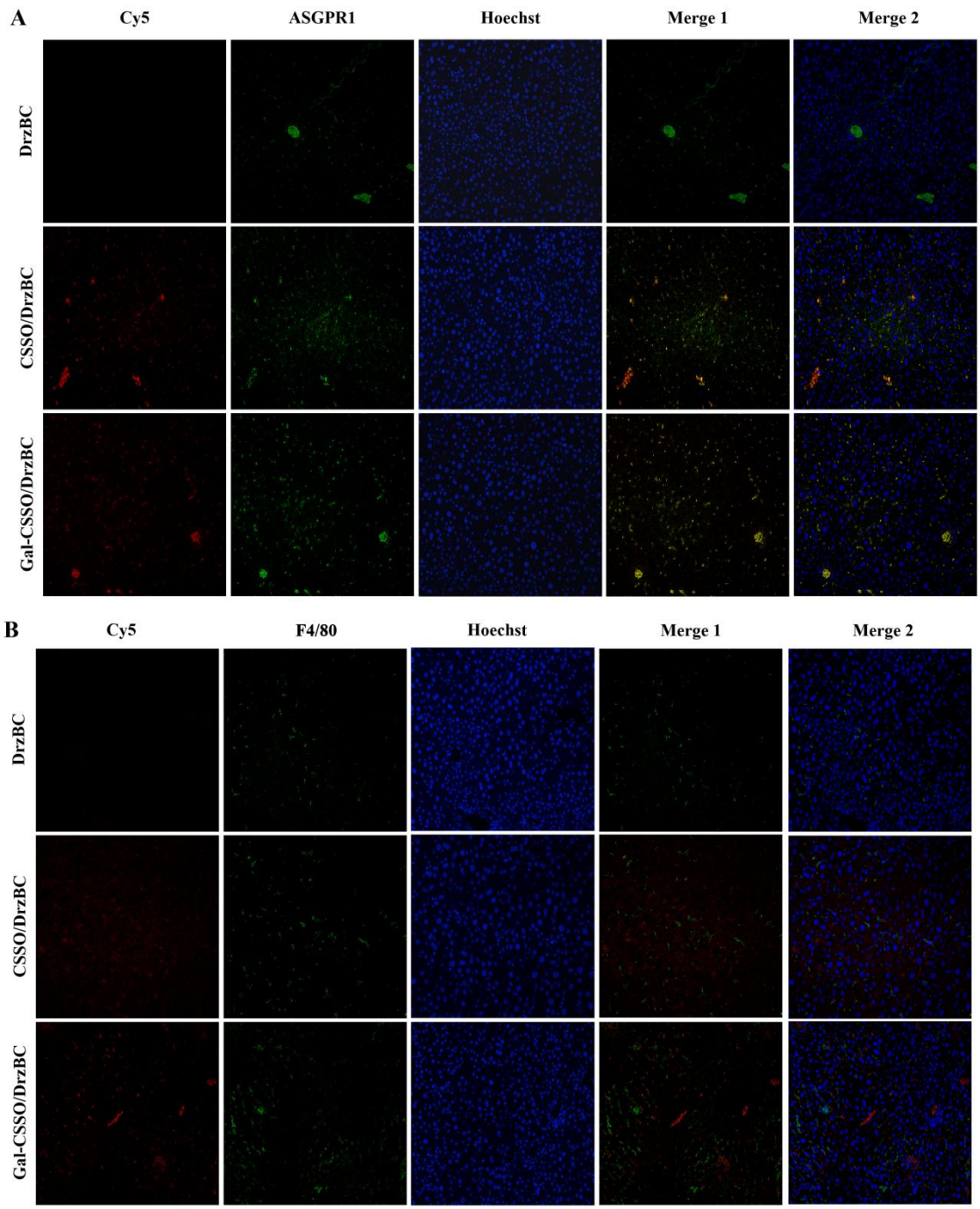

Figure S4. Confocal laser scanning microscopy images of hepatocytes (HCs) (A) and Kupffer cells (KCs) (B) that absorbed DrzBC, CSSO/DrzBC, and Gal-CSSO/DrzBC after i.v. injection for 12 h (×200). DrzBC was labeled using Cy5 (red), HCs were labeled using anti-ASGPR1 and -BV421 (green), KCs was labeled using PE/Cy7 anti-mouse F4/80 (green), and nuclei were stained with DAPI.

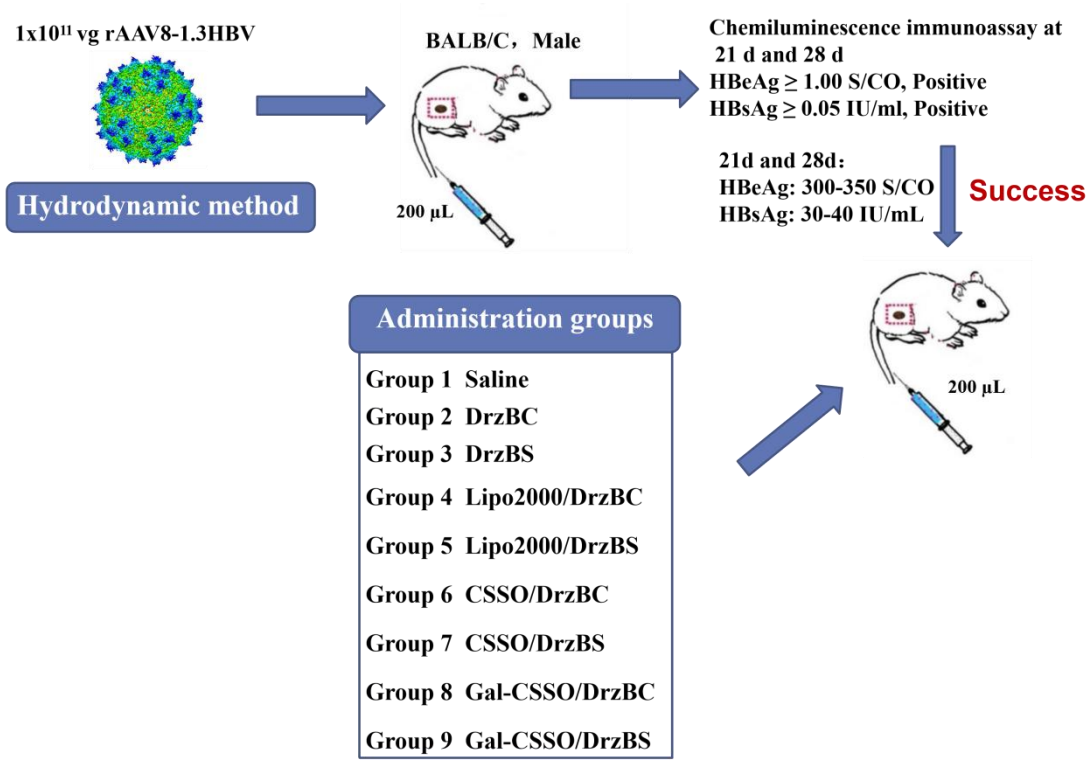

Figure S5. Scheme for constructing and evaluating HBV-infected mice.